Some Considerations on the Prediction of Fatigue Crack Growth Retardation in Structural Materials

M. V. Pereira[1], F.A. Darwish[2], A. F. Camarão[3] and S. H. Motta[4]
[1]PUC-Rio, Rio de Janeiro, Brazil; [2]UFF, Niterói, Brazil;
[3]Arvin-Meritor, Osasco, Brazil; [4]Brasilamarras, Niterói, Brazil

The purpose of this work is to evaluate the applicability of the Willenborg model to predicting residual fatigue life extension in an R3 grade structural steel and a 7150 T7 aluminum alloy. Compact tension specimens were subjected to a single overload during constant amplitude loading and crack propagation rate *da/dN* was monitored as a function of the stress intensity factor range ΔK. The size of the delay zone as well as the number of the delay cycles were predicted by the model and then compared with the experimental data. Whereas the predicted delay zone size was found to be in good agreement with the experimental observations, the application of the model to predict the retardation factor may lead, depending on the intensity of overloading, to under- or overestimating crack propagation rate within the delay zone. This, in turn, could result in an imprecise estimate of the delay cycles number and hence of the residual fatigue life.

1. Introdution

Structural and mechanical components when in service under cyclic loading may be subjected to either variable amplitude loading or occasional overload cycles and these load interactions complicate life prediction. However, overload cycles of sufficient magnitude can be applied with the purpose of extending fatigue life, as they result in a transient retardation in the rate of fatigue crack growth at the baseline level [1]. Following an overload cycle, the fatigue crack starts to advance into the overload (OL) plastic zone and the residual compressive stresses in an element just behind the crack tip are relaxed. This contributes to the level of crack closure in the wake of the crack tip, thus retarding fatigue crack propagation. As the crack exits the OL plastic zone, the propagation rate is generally back again at the baseline level corresponding to the constant amplitude (CA) loading [2].

The magnitude and extent of crack growth retardation due to the imposition of a single OL during CA cycling are usually measured by parameters such as the delay cycles number N_d and the delay zone size Δa_d. The first parameter refers to the increase in residual fatigue life due to overloading and the second is a measure of the OL affected crack length increment along which retardation takes place. Both N_d and Δa_d can vary depending on load parameters [3]. For example, the higher the ratio between the magnitude of the overload and that of the CA maximum load, R_{OL}, the more pronounced the crack growth retardation. That is, an increase in R_{OL} results in an increase in N_d and Δa_d, as well as in a decrease in the minimum *da/dN* level [3]. For high overloads (R_{OL} = 2.5) the initial crack growth acceleration that immediately follows an overload was absent and immediate retardation was observed [4,5].

In regard to the effect of the CA load ratio R, defined by the ratio between the minimum ($K_{\min}$) and maximum ($K_{\max}$) stress intensity factors, crack growth retardation was found to decrease with the increase in R. The increase in R was also accompanied by a decrease in the fatigue crack length increment between the OL application and the occurrence of the minimum da/dN [5-7]. Initial growth acceleration was found to vanish and retardation became immediate for high R values around 0.6 [6]. Another interesting observation refers to the fact that the ratio of Δa_d to the size of an OL plastic zone, developed under plane stress conditions, was found to decrease as R increases. Typically, this ratio is expected to vary from 3.5 at $R = 0.1$ to values ranging between 0.2 and 0.3 for $R = 0.45$. That is, depending on loading conditions, the delay zone size can be much larger or smaller than the OL monotonic plastic zone size calculated for plane stress conditions [4,6,8].

In addition to the loading parameters, material properties also have a considerable bearing on fatigue crack growth retardation following a single overload. Several works [9,10] have shown that the higher the yield stress, the more short-termed becomes the overall retardation effect.

Starting early seventies, a large number of models which incorporate interaction effects have been introduced for predicting fatigue crack growth under variable amplitude (VA) loading [11-17]. These models are characterized by introducing crack tip plasticity effects and they comprise three distinct groups. The yield zone models are based on considerations on the size of monotonic plastic zone created at the crack tip due to an OL and do not take into account plasticity induced crack closure due to the imposition of the overload. Crack closure models, on the other hand, represent an improvement of the more primitive yield zone models and take into consideration the closure behavior based on crack closure measurements made during CA loading [18]. Assumptions are then made about the crack closure behavior under VA loading. In the more sophisticated strip yield models, the occurrence of plasticity induced crack closure is calculated rather than estimated from measurements made during CA loading [18].

The present study has the purpose of applying the Willenborg model, which belongs in the yield zone models, in order to predict fatigue life extension due to a single overload cycle applied at a given crack length during CA loading. The materials chosen for carrying out the fatigue tests were an R3 grade structural steel largely used for fabricating offshore mooring chains and a 7150 T7 aluminum alloy developed for aeronautic applications. The study was motivated by the simplicity of the model in question and was primarily aimed at comparing the delay parameters predicted by its application with experimental data.

2. Basic Feature of the Willenborg Model

The model proposed by Willenborg [13] is based on the assumption that crack growth delay after an OL is due to a reduction in K_{max}, corresponding to the current crack length. According to the model, the reduction in K_{max}, K_{red}, is given by [13]:

$$K_{red} = K_{req} - K_{max} \quad (1)$$

where K_{req} is the stress intensity factor necessary to produce a plastic zone that extends a distance λ ahead of the advancing fatigue crack tip, to the far edge of the OL plastic zone, as presented in Fig. 1. Under plane stress conditions, K_{req} at a given crack length a can be determined from the expression:

$$K_{req} = \sigma_Y \sqrt{\pi\lambda} \quad (2)$$

where λ , as shown in Fig.1, is given by:

$$\lambda = a_0 + (r_p)_{OL} - a \quad (3)$$

where a_0 is the crack length at which the overload was applied and $(r_p)_{OL}$ is the corresponding plastic zone size that can be calculated for plane stress loading, using the following expression:

$$(r_p)_{OL} = \frac{1}{\pi}\left(\frac{K_{OL}}{\sigma_Y}\right)^2 \quad (4)$$

where K_{OL} is the OL stress intensity factor calculated according to literature [12,19].

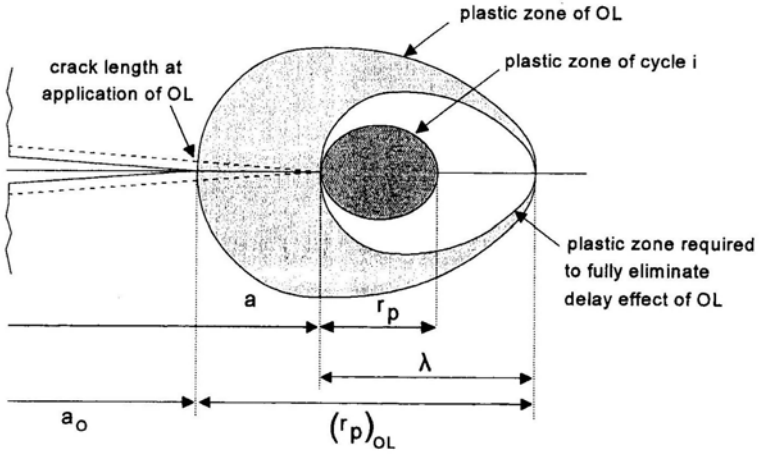

Figure 1. Plastic zone size definitions used in the model of Willenborg, corresponding to a generic cycle *i* [18].

Taking into account the reduction in the stress intensity factor due to overloading, one can define effective values of K_{max} and K_{min} as follows:

$$K_{max,eff} = K_{max} - K_{red} \quad (5)$$

$$K_{min,eff} = K_{min} - K_{red} \quad (6)$$

From the effective stress intensity levels given above, one can, in turn, define in the usual manner the effective stress intensity factor range, ΔK_{eff}, as well as the effective stress intensity factor ratio R_{eff}. At this point, it is important to note that Eqs. (5) and (6) indicate that ΔK_{eff} is equivalent to ΔK. However, according to the Willenborg model, negative values of $K_{min,eff}$ should be taken as null and ΔK_{eff} becomes equal to $K_{max,eff}$ in this case.

Knowing ΔK_{eff} and R_{eff}, the fatigue crack propagation rate $(da/dN)_{VA}$ within the delay zone can be estimated and then related to the corresponding propagation rate at the baseline level $(da/dN)_{CA}$ by the retardation factor γ defined as:

$$(da/dN)_{VA} = \gamma\,(da/dN)_{CA} \tag{7}$$

Fatigue crack growth rate under CA loading can be predicted from the relation proposed by Forman and co-workers [20], as shown in Eq. (8):

$$\left(\frac{da}{dN}\right)_{CA} = \frac{C(\Delta K)^n}{(1-R)K_c - \Delta K} \tag{8}$$

where C and n are the Paris law material constants and K_c is the material's toughness.

Within the delay zone that follows the application of an OL, the crack propagation rate $(da/dN)_{VA}$ can be calculated by substituting ΔK_{eff} and R_{eff} for ΔK and R in Eq. (8). After passing through the minimum that follows an overload, the retardation factor γ starts to increase and eventually becomes equal to unity, thus restoring the propagation rate back to the baseline level at the end of the delay zone. The basic feature of the Willenborg model, therefore, refers to the fact that crack growth retardation, which follows overloading, ends when the values of ΔK_{eff} and R_{eff} converge to those of ΔK and R. The current crack length, a^*, at which such convergence takes place can thus be determined and the delay zone size Δa_d^* will be given by the difference between a^* and a_0.

Based on Eq. (8), $(da/dN)_{CA}$ and $(da/dN)_{VA}$ can be calculated and the delay factor γ for a given crack length a can, therefore, be expressed as:

$$\gamma = \left(\frac{\Delta K_{eff}}{\Delta K}\right)^n \left[\frac{(1-R)K_c - \Delta K}{(1-R_{eff})K_c - \Delta K_{eff}}\right] \tag{9}$$

3. Materials and Experimental

The materials used for this investigation were an R3 grade structural steel and a 7150 T7 aluminum alloy. The steel, which contains, in weight percent, 0.26% C, 1.2% Cr, 1.75% Mn, 0.35% Ni, was received in the form of hot rolled round bars of circular cross section with a nominal diameter of 85 mm. The aluminum alloy was received in the form of an extruded T-profiled rod containing, in weight percent, 6.6% Zn, 2.3% Mg, 2.1% Cu, 0.1% Zr, 0.05% Fe, 0.05% Ti, 0.03% Si and traces of Mn and Cr.

Compact tension (CT) specimens were machined from the as-received steel bars along the L-T orientation, in accordance with the ASTM E647-99 recommendation [19]. A number of CT specimens were also machined from the steel after it was heat treated by austenitization at 900ºC during 90 minutes, followed by water quenching and then tempering at 600ºC for 90 minutes. Other CT specimens were cut off from the as-received aluminum alloy along the rod´s L-T orientation, according to the same ASTM recommendation. The study was, therefore, carried out contemplating three different microstructures: as-received (SA) and heat treated (SH) R3 grade steel, as well as extruded 7150 aluminum alloy (AL). Table 1 indicates the yield stress (σ_Y) and fracture toughness (K_c) as determined for the 8 mm thick CT specimens. It is clear from this table that, whereas K_c values of the aluminum alloy satisfy the ASTM criterion for plane strain conditions, this is not the case for the steel in both conditions.

Table 1. Materials properties

Material	σ_Y (MPa)	K_c (MPa$\sqrt{m}$)
SA	530	101
SH	545	109
AL	565	24

The specimen width (W) and specimen thickness were taken as 32 and 8 mm, respectively, and a starter notch was machined to a depth of 7 mm. The specimen surfaces were polished and fine lines were drawn parallel to the specimen axis in order to facilitate monitoring crack growth during cyclic loading. Finally, the CT specimens were precracked to a total crack length-to-specimen width ratio, *a*/W, of about 0.27.

CA cyclic loading was applied to the precracked specimens so as to obtain the typical *da/dN* versus *ΔK* curves for the materials in question. The tests were performed at room temperature using a servo-hydraulic machine, operated at a frequency of 20 Hz. The CT steel specimens were submitted to a tension-tension mode I loading with a maximum load of 9 kN and a load ratio of 0.33. For the aluminum alloy specimens, the maximum load was taken as 2.1 kN and the *R* ratio as 0.3. Fatigue crack length was monitored using a traveling microscope.

Overload cycles were applied manually under load control at an *a*/W equivalent to 0.33 and 0.4 for the steel and aluminum alloy specimens, respectively. The overload ratio R_{OL}, defined by K_{OL} / K_{max} [21], was taken as 1.5 and 1.8 for the steel and 1.5, 1.75 and 2 for the aluminum alloy.

4. Results and Discussion

Following the application of single overloads during CA fatigue testing, the maximum retardation in crack propagation is reached only after a small crack length increment [18]. After passing the point of maximum retardation, defined by $\gamma = \gamma_{\min}$, *da*/*dN* starts to increase and eventually returns, over some crack extension Δa_d, to the normal growth rate at the CA baseline level. The values of

Δa_d, together with those of $\gamma_{\min}$, are presented in Table 2 for the test conditions considered in this work. The numbers listed in this table indicate, as one may expect, that an increase in the overload ratio is associated with an increase in Δa_d and a decrease in $\gamma_{\min}$. This, in turn, is reflected, as Table 2 indicates, in an increase in the delay cycles number N_d and hence in the residual fatigue life.

Table 2. Delay parameters determined for the different test conditions

Material	R_{OL}	$\gamma_{\min}$	Δa_d *(mm)*	$(r_p)_{OL}$ *(mm)*	N_d
SA	1.50	0.39	1.50	3.60	10160
	1.80	0.20	2.00	5.16	26740
SH	1.50	0.52	1.30	3.39	10880
	1.80	0.21	2.00	4.88	30370
AL	1.50	0.20	0.20	0.25	4660
	1.75	0.12	0.26	0.34	7640
	2.00	0.04	0.36	0.44	18007

The values of the corresponding OL plastic zone size, calculated using Eq. (4), are listed in Table 2, for the purpose of comparison with those of Δa_d. At this point, it is important to mention that, as the measurements of crack length were made on the specimen surface, the use of Eq. (4), which corresponds to plane stress condition, is considered to be appropriate. As can be verified from the same table, the ratio between Δa_d and $(r_p)_{OL}$ varies between 0.38 and 0.41 for the steel specimens that were fatigue tested at an R ratio of 0.33. This is seen to be in agreement with published data [4,6,8] where Δa_d was reported to be 20 → 30% the size of the overload plastic zone for R equal to 0.45. For the aluminum base alloy, on the other side, an R ratio of 0.3 was adopted for fatigue testing and this implied in a $\Delta a_d / (r_p)_{OL}$ ratio varying between 0.76 and 0.81, which is considered in fair agreement with what is reported in the literature [4,6,8].

Another observation worthy of mentioning refers to the fact that the heat treatment, to which the steel was submitted, results in a decrease of the delay zone size Δa_d. Presumably, this can be attributed to the increase in the yield stress of the material, implying in a more short-termed retardation effect [9,10].

4.1 Application of the Model

The application of the Willenborg model is based on determining the crack length a^*, at which ΔK_{eff} and R_{eff} converge to ΔK and R. The values of a^* thus obtained are presented in Table 3, for the test conditions considered in this study.

The corresponding ΔK value, denoted ΔK^*, the extent of the delay zone Δa_d^* and the experimental counterpart Δa_d are also presented in Table 3. As this table

indicates, Δa_d^* agrees fairly well with Δa_d and hence one may use the Willenborg model to predict the extent of the delay zone resulting from overloading. In regard to the retardation factor, as predicted by the model, the values of γ can be calculated from Eq. (9), taking the Paris law exponent as 2 and 3.8 for the steel and aluminum base alloy, respectively.

Table 3. Values of a^* and ΔK^* as predicted by the Willenborg model

Material	R_{OL}	a^* (mm)	ΔK^*(MPa$\sqrt{m}$)	Δa_d^* (mm)	Δa_d (mm)
SA	1.50	12.00	28.31	1.50	1.50
	1.80	13.10	30.85	2.60	2.00
SH	1.50	12.00	28.31	1.50	1.30
	1.80	13.10	30.85	2.60	2.00
AL	1.50	12.94	7.46	0.14	0.21
	1.75	13.03	7.51	0.23	0.28
	2.00	13.10	7.56	0.30	0.36

Examples of the comparison of the predicted γ_c values with those experimentally detected γ_e are shown in Table 4 for the SA, SH and AL test conditions, corresponding, respectively, to overload ratios of 1.5, 1.8 and 2. One can observe the good agreement between γ_c and γ_e values for R_{OL} of 1.5. However, for higher overload ratios, γ_c is seen to be generally lower than its experimental counterpart γ_e and, as expected, they both converge to unity as the fatigue crack heads towards the end of the delay zone.

At this point one should mention that the results obtained in the present study indicate that the relationship between γ_c and γ_e as described above is in fact typical of the steel behavior for the different test conditions. In regard to the aluminum alloy, the application of the Willenborg model for the lower R_{OL} ratios results in understimating the retardatin effect, giving rise to higher γ_c in comparison to those of γ_e. Accordingly, it can be concluded that the applicability of the Willenborg model to predicting the retardation factor following overloading depends on the magnitude of the applied overload.

4.2 Prediction of the Residual Fatigue Life Extension

The extension of the residual fatigue life due to the application of a single overload can be estimated from the expression:

$$N_d^* = \int_{a_0}^{a^*} \frac{da}{\gamma_c \, (da/dN)_{CA}} - \int_{a_0}^{a^*} \frac{da}{(da/dN)_{CA}} \qquad (10)$$

where N_d* is the delay cycles number and a* the crack length at which the crack propagation rate is restored back to the base line level. Knowing the values of $(da/dN)_{CA}$ at different crack length increments within the delay zone, one can numerically evaluate the integrals in the above equation and hence calculate N_d*.

Table 4. Experimental and Willenborg-predicted values of the retardation factor

Material	R_{OL}	a (mm)	$(da/dN)_{CA}$	γ_c	γ_e
SA	1.5	10.5	$8.0\text{x}10^{-4}$	1	1
		11.0	$8.2\text{x}10^{-4}$	0.39	0.39
		11.5	$8.7\text{x}10^{-4}$	0.72	0.72
		12.0	10^{-4}	1.00	1.00
SH	1.8	10.5	$6.6\text{x}10^{-5}$	1.00	1.00
		11.0	$7.1\text{x}10^{-5}$	0.21	0.21
		11.5	$9.4\text{x}10^{-5}$	0.23	0.34
		12.0	10^{-4}	0.56	0.87
		12.5	$1.1\text{x}10^{-4}$	0.70	0.90
		13.0	$1.3\text{x}10^{-4}$	0.95	0.95
		13.1	$1.3\text{x}10^{-4}$	1.00	1.00
AL	2.0	12.80	$4.54\text{x}10^{-5}$	1.00	1.00
		12.94	$5.38\text{x}10^{-5}$	0.04	0.03
		13.00	$5.74\text{x}10^{-5}$	0.19	0.52
		13.02	$5.86\text{x}10^{-5}$	0.31	0.64
		13.04	$5.98\text{x}10^{-5}$	0.48	0.76
		13.06	$6.10\text{x}10^{-5}$	0.61	0.84
		13.10	$6.34\text{x}10^{-5}$	1.00	1.00

Based on the data presented in Table 4, delay cycles numbers of 11772, 50287 and 51314 were obtained for the test conditions indicated in the table. Comparing these numbers with their respective N_d values listed in Table 2, one can conclude that the Willenborg model is fairly precise in predicting residual fatigue life extension at R_{OL} = 1.5 and up to 1.75 for the aluminum alloy. For higher ratios, though, the use of the model implies in overestimating the delay cycles number, in virtue of the low predicted values of γ_c. A complete comparison between N_d and N_d* is presented in Table 5, for all the conditions in question.

Table 5. Experimental and predicted values of the delay cycles numbers

Material	R_{OL}	N_d	N_d*
SA	1.5	10160	11772
	1.8	26740	53916
SH	1.5	10880	8105
	1.8	30370	50287
AL	1.50	4660	3330
	1.75	7640	5347
	2.00	18007	51314

5. Concluding Remarks

The purpose of the present work was to evaluate the applicability of the Willenborg model to predicting fatigue crack growth retardation in structural materials. From what is presented above, the following remarks can be made:

- An increase in the overload ratio during CA loading results in a more effective crack growth retardation as evidenced by the increase in the extent of the delay zone and by a decrease in the retardation factor.
- The extent of the retardation zone predicted by the Willenborg model agrees fairly well with the experimental observations.
- The applicability of the model to predicting the retardation factor depends on the level of overloading. While, in the present study, this prediction was found to be fairly precise for an overload ratio of 1.5, the model overestimates the retardation effect due to higher overload ratios of 1.8 for steel and 2 for aluminum base alloy.
- The delay cycles numbers predicted by the model were found to be in fair agreement with those observed experimentally for the low overload ratio (R_{OL} = 1.5). The model, though, overestimates residual fatigue life extension for higher overload ratios of 1.8 for steel and 2 for aluminum base alloy.

REFERENCES

[1] J. Schijve, Fatigue crack propagation in light alloy sheet materials and structures, Report No. MP-195, National Luchtvaart Laboratorium, Delft, 1960.
[2] A.J. McEvily, S. Ishihara, On the retardation in fatigue crack growth rate due to an overload: a review, in: P.M. Pimenta, L.C.H. Ricardo, A.F. Camarão (Eds.), Modern Trends on Fatigue, SAE Brazil, São Paulo, 2001, pp. 145-150.
[3] M. Skorupa, Load interaction effects during fatigue crack growth under variable amplitude loading – a literature review. Part I: empirical trends, Fatigue Fract Engng Mater Struct 21 (1998) 987-1006.
[4] C.M.Ward-Close, A.F. Blom, R.O. Ritchie, Mechanisms associated with transient fatigue crack growth under variable-amplitude loading: An experimental and numerical study, Engng Fract Mech 32 (1989) 613-638.
[5] D. Damri, J.F. Knott, Transient retardation in fatigue crack growth following a single peak overload, Fatigue Fract Engng Mater Struct 14 (1991) 709-719.

[6] C.S. Shin, S.H. Hsu, On the mechanisms and behaviour of overload retardation in AISI 304 stainless steel, Int J Fatigue 15 (1993) 181-192.
[7] H. Tsukuda, H. Ogiyama, T. Shiraishi, Transient fatigue crack growth behaviour following single overloads at high stress ratios, Fatigue Fract Engng Mater Struct 19 (1996) 879-891.
[8] D.M. Shuter, W. Geary, Some aspects of fatigue crack growth retardation behaviour following tensile overloads in a structural steel, Fatigue Fract Engng Mater Struct 19 (1996) 185-199.
[9] C. Robin, M. Louah, G. Pluvinage, Influence of the overload on the fatigue crack growth in steels, Fatigue Fract Engng Mater Struct 6 (1983) 1-13.
[10] G.L. Chen, R Roberts, Delay effects in AISI 1035 steel, Engng Fract Mech 22 (1985) 201-212.
[11] O.E. Wheeler, Spectrum loading and crack growth, J Basic Eng. 94 (1972) 181-186.
[12] D. Broek, Elementary engineering fracture mechanics, Kluwer Academic Publishers, Dordrecht, 1986.
[13] J. Willenborg, R.M. Engle, H.A. Wood, A crack growth retardation model using an effective stress concept, AFFDL-TR71-1, Air Force Flight Dynamic Laboratory, Dayton, 1971.
[14] G. Baudin, M. Robert, Crack growth life time prediction under aeronautical type loading, in: L. Faria (Ed.), Life assessment of dynamically loaded materials and structures, Engineering Materials Advisory Services Ltd., Warley, 1985, pp. 779-792.
[15] T.H. Topper, D.L. DuQuesnay, The effects of overloads in service load histories on crack closure and fatigue damage, in: P.M. Pimenta, L.C.H. Ricardo, A.F. Camarão (Eds.), Modern Trends on Fatigue, SAE Brazil, São Paulo, 2001, pp. 43-54.
[16] J.E. Allison, The measurement of crack closure during fatigue crack growth, in: D.T. Read, R.P. Reed (Eds.), ASTM STP 945, American Society for Testing and Materials, Philadelphia, 1988, pp. 913-933.
[17] G.S. Wang, A.F. Blom, A strip model for fatigue crack growth predictions under general load conditions, Eng Fract Mech 40 (1991) 507-533.
[18] J. Schijve, Fatigue of structures and materials, Kluwer Academic Publishers, Dordrecht, 2001.
[19] ASTM, Standard test method for measurements of fatigue crack growth rates, ASTM E647-01, American Society for Testing and Materials, Philadelphia, 2001.
[20] R.G. Forman, V.E. Kearney, R.M. Engle, Numerical analysis of crack growth propagation in loaded structures, J Basic Eng 89 (1967) 459-464.
[21] X. Decoopman, A. Imad, M. Nait-Abdelaziz, G. Mesmacque, Effect of baseline loading on fatigue crack growth retardation due to an overloading, in: M.W. Brown, E.R. de los Rios, K.J. Miller KJ (Eds.), Fracture from Defects, Engineering Materials Advisory Services Ltd., Warley, 1998, pp. 265-270.